STUDIA UBB CHEMIA, LVII, 3, 2012 (p. 223 – 236)
(RECOMMENDED CITATION)

ANODIC DISSOLUTION OF SOME ELECTRODE MATERIALS INVOLVED IN ELECTROCHEMICALLY ASSISTED COAGULATION

MARIUS SEBASTIAN SECULA[1], GHEORGHE NEMTOI[2], IGOR CRETESCU

ABSTRACT. A study approaching the anodic dissolution of iron and aluminum based electrodes in aqueous solutions containing sulfate or chloride ions is presented in this paper. Beside the influence of the supporting electrolyte, it is experimentally established the influence of the solution pH on the anodic dissolution of the two anodic materials considered. As the anodic dissolution of the anode surface is the first step of electrocoagulation processes, the results obtained are important in order to achieve a better understanding of these processes. The anodic dissolution process depends mainly on the specific electrical charge passed. Current density at null potential, heterogeneous constant rate in mixed regime and dissolution rate are determined. The influence of mass transport over the global rate of the dissolution rate of aluminum and iron respectively is established.

Keywords: *electrocoagulation, anodic dissolution, iron, aluminum, corrosion parameters*

INTRODUCTION

In the last decades, electrochemical technologies of wastewater treatment have been undergoing intensive development. Among these technologies, one of the most promising is electrochemically assisted coagulation that can compete with the conventional chemical coagulation process in the treatment of wastewaters [1,2].

In electrocoagulation, an electrochemical cell is used to provide aluminum or iron ions into the wastewater. Depending on the pH conditions and wastewater chemistry, these ions destabilize the colloidal pollutants, similarly to the case of conventional coagulation process. The turbulence

[1] *TUIASI - "Gheorghe Asachi" Technical University, Faculty of Chemical Engineering and Environmental Protection, 73 Prof. Dr. docent D. Mangeron, 700050, Iasi, Romania, mariussecula@ch.tuiasi.ro*
[2] *"Al. I. Cuza" University, Faculty of Chemistry, 11 Carol I, 700506, Iasi, Romania*

generated by the oxygen and the hydrogen evolution generates a soft mix that helps the destabilized colloids to flocculate (to link together and to generate bigger particles). Finally, the pollutants are removed from the wastewater by sedimentation, filtration or flotation [3].

Although, electrocoagulation is a rather old technology, it has received very little scientific attention. Only in the last few years, some works focused on the study of electrocoagulation technology and especially on the fundamental principles lying at its basis [4,5]. Nevertheless, to make this technology competitive, a better understanding of the involved processes has to be achieved. Canizares et al. [5-7], in case of aluminum anode, and Noubactep and Schoner [8], in case of iron anode, investigated the mechanisms of electrocoagulation with a special regard to the speciation of the dissolved metals. Recently, Mouedhen et al. [9] reported several results on the corrosion of aluminum in the presence of NaCl, in the range of 0-1.7 mM. However, according to our knowledge mass transport phenomena taking place at the anode surface under the condition specific to electrocoagulation systems have not been addressed yet. In spite of numerous studies reported on the corrosion of both aluminum and iron in the presence of the two considered background electrolytes, there is no systematic approach of these systems with regard to the electrocoagulation technique.

The main purpose of this work is to study the anodic dissolution of iron and aluminum into diluted aqueous solutions. The characterization of the first step of electrocoagulation is of very high importance in order to achieve a thorough understanding of the whole process. Linear sweep voltammetry was employed to characterize the dissolution process of aluminum and iron in diluted aqueous solutions of sodium chloride or sodium sulfate. By using the potentiodynamic polarization curves on a wide potential range, the limiting rates of the investigated anodic dissolution processes were established. The method of linear polarization resistance, Evans diagrams and Stern's second method were used to estimate the values of corrosion currents that define the specific dissolution process. Also, values of dissolution rate of the anodic dissolution processes taking place under kinetic and mixed regimes at various potential values were calculated.

THEORY

It is well known that in order to generate coagulant into an electrocoagulation reactor, it is necessary to apply a potential difference between electrodes. Occurring electrode reactions depend on the operating pH and species present in the electrochemical system. The electrode material generates the type of coagulant cation and thus, the electrochemical reactions.

Electrocoagulation literature describes the following reactions taking place at the anode and cathode [3]:

At the anode:

$$M_{(s)} \rightarrow M_{(aq)}^{n+} + ne^- \quad (1)$$

$$2H_2O_{(l)} \rightarrow O_{2(g)} + 4H_{(aq)}^{+} + 4e^- \quad (2)$$

At the cathode:

$$2H_2O_{(l)} + 2e^- \rightarrow H_{2(g)} + 2OH^-_{(aq)} \quad (3)$$

These reactions explain the appearance of bubbles near the cathodes and anodes during the process and can also explain the consequent increase of pH (dependent on the solution alkalinity and electrochemical process rate, i.e., the intensity of the electric current and operation time).

When iron or aluminum electrodes are involved, the generated $Fe_{(aq)}^{2+}$ or $Al_{(aq)}^{3+}$ ions will immediately undergo further spontaneous reactions to produce the corresponding hydroxides and/or polyhydroxides [6,10].

Throughout the anodic range of the polarization curves there might be identified several energetic areas (potential ranges) where electrode materials emphasize certain behaviors. Thus, in certain potential ranges the metal material is strongly corroded, while, in others, the electrode becomes passivated.

Based on the linear polarization curves, important parameters of anodic dissolution process such as corrosion and passivation potentials and their corresponding current densities can be determined [11].

Cyclic potentiodynamic curves might present a hysteresis that describes the material tendency toward a certain type of corrosion (intergranular, pitting, crevice etc.) [12].

Steady-state polarization consists in applying of a potential difference between reference electrode and working electrode. When the steady-state is reached, the current response is recorded.

The process kinetics is strongly influenced by the electrode potential and is described by the Butler-Volmer equation that can be simplified for two extreme cases [12].

For a high value of the overpotential, the reaction becomes irreversible and consequently one of the exponential terms becomes insignificant. Therefore, Butler-Volmer equation can be simplified to [11]:

$$\ln|i| = \ln i_0 + \frac{\alpha \cdot n \cdot F}{R \cdot T}\eta \quad (4)$$

According to Stern's first method [13,14], Tafel slope leads to the value of charge transfer coefficient, α, while the intercept leads to the value of exchange current, i_0.

However, at high values of polarization potential, the corresponding current can dissolve the metal or might reduce some superficial films on the electrode. These might influence the interphase state and the values of corrosion rates [15].

Stern's second method avoids these deficiencies due to the determination of corrosion current takes also into account the polarization resistance [16]. For a low variation of the potential, Butler-Volmer equation becomes [16]:

$$i = i_0 \frac{n \cdot F}{R \cdot T} \eta \tag{5}$$

where is overpotential, i_0 – the exchange current, R – gas constant, T – temperature, F – Faraday's constant and n – number of electrons.

Current-overpotential relationships allow one to determine the exchange current density, i_0, also named the corrosion current density, when the corrosion process takes place.

Corrosion potential can be determined from the polarization curves by means of Evans plots (logarithm of current density vs. overpotential) [17].

Resistance to exchange transfer was calculated using the following equation:

$$R_p = \frac{R \cdot T}{n \cdot F \cdot I_0} \tag{6}$$

The rate of an anodic dissolution process is defined by the relationship [18]:

$$v_D = \frac{dm_O}{S \cdot dt} \tag{7}$$

where m is the quantity of species O, kg; S – cross section area normal to the ax of mass flow, m^2. Taking into account Farraday's laws, eq. (7) becomes:

$$v_D = \frac{M_O \cdot i}{n \cdot F} \tag{8}$$

RESULTS AND DISCUSSION

Aluminum dissolution in diluted aqueous solution containing NaCl

Fig. 1a shows several sweep linear voltammograms obtained at aluminum dissolution into sodium chloride of different pH. These voltammograms were used to determine the polarization resistance, according to eq. (6), corrosion currents, by means eq. (5), and Tafel corrosion currents, based on eq. (4). Considering current values at different relative electrode potentials, aluminum dissolution rates were calculated with eq. (8) in order to point out the intensity of the dissolution process taking place at various values of pH.

Fig. 1a pinpoints that the slopes of current-potential dependences present no significant change throughout a relative wide potential range. This means the current is not limited by mass transfer. Therefore, the electrochemical reaction is the limiting rate.

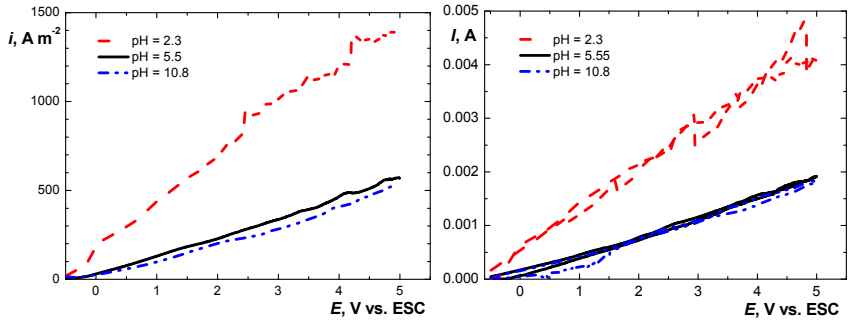

(a) (b)

Figure 1. Linear sweep (a) and cyclic (b) voltammograms of aluminum anode – 3.42 mM NaCl system at three values of pH. Potential ranges: -0.5 – 5 V/ESC and -0.5 – 5 -0.5 V/ESC; sweep rate 50 mV·s^{-1}; Resolution time 0.8 s, T = 298 K, anode diameter 2.07 mm

Cyclic voltammograms (Fig. 1b) present a small hysteresis. However, it is obvious that on these ranges of the potential the corrosion phenomena occur at all three values of pH. In case of acid medium, several bounces of the current can be noticed. These may be explained by the detachment of oxygen bubbles formed onto the electrode surface. The competition between aluminum dissolution and oxygen evolution leads to a decrease in aluminum generation efficiency [4].

According to the studies performed by Macdonald [19], the corrosion current increases with the potential sweep rate. As listed in Table 1, in case of aluminum dissolution in diluted aqueous solution of NaCl with a pH of 5.5, the increase of corrosion current with sweep rate is valid for both calculation methods of corrosion current. In Fig. 2 are shown Evans plots for aluminum dissolution in sodium chloride solution at various values of pH (Fig. 2a), and sweep rates of potential (Fig. 2b). Then, the values of corrosion current were determined according to the second method of Stern.

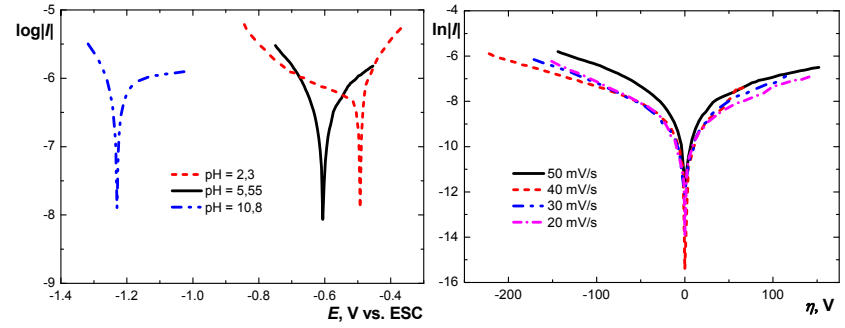

(a) (b)

Figure 2. Semi logarithmic I-η plot of aluminum dissolution in sodium chloride solution (a) at various pH values and (b) at various sweep rates of potential, pH = 5.5

Table 1. Corrosion parameters of Al÷3.42 mM NaCl system at various sweep rates and different values of pH

Run No.	pH	Potential range	Sweep rate	E_{cor}	$I_{O,\ init}$	R_p	$I_{O,\ Tafel}$	$i_{O,\ Tafel}$
		V vs. ESC	$mV \cdot s^{-1}$	V	A	$\Omega \cdot m^2$	A	$A \cdot m^{-2}$
1	5.5	–0.15 ÷ 0.15	50	-0.514	$2.641 \cdot 10^{-07}$	0.108	$2.392 \cdot 10^{-07}$	0.071
2	5.5	–0.15 ÷ 0.15	40	-0.525	$4.818 \cdot 10^{-08}$	0.590	$8.378 \cdot 10^{-08}$	0.025
3	5.5	–0.15 ÷ 0.15	30	-0.525	$4.643 \cdot 10^{-08}$	0.612	$7.421 \cdot 10^{-08}$	0.022
4	5.5	–0.15 ÷ 0.15	20	-0.587	$4.362 \cdot 10^{-08}$	0.652	$6.919 \cdot 10^{-08}$	0.021
5	2.3	–0.5 ÷ 5	50	-0.595	$2.52 \cdot 10^{-08}$	1.127	$1.296 \cdot 10^{-06}$	0.385
6	5.5	–0.5 ÷ 5	50	-0.601	$8.41 \cdot 10^{-08}$	0.338	$2.040 \cdot 10^{-07}$	0.061
7	10.8	–0.5 ÷ 5	50	-1.170	$5.11 \cdot 10^{-08}$	0.556	$1.684 \cdot 10^{-07}$	0.050

As can be noticed, in strong acid medium aluminum dissolution is more pronounced, and Tafel corrosion current is one order of magnitude higher than the corrosion currents obtained for this system in alkaline medium as emphasized in Fig. 1a. The obtained results are in agreement with those reported by Mouedhen et al. [9]. In the presence of chloride ion enhances the pitting corrosion phenomena onto the metal surface [20].

Fig. 3 shows the variation of dissolution rate of aluminum in solution containing chloride ion at different values of electrode potential and pH.

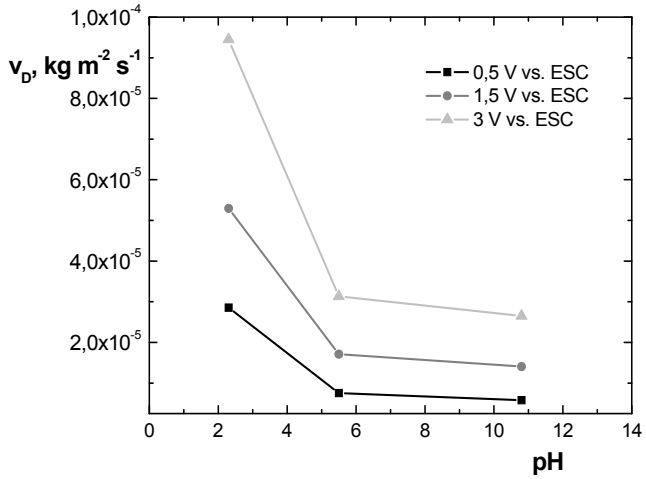

Figure 3. Dependence of aluminum dissolution rate on the solution pH

The acid pH favors the dissolution process, and the dissolution rate of aluminum increases proportionally with the potential for all pH values.

Aluminum dissolution in diluted aqueous solution containing Na_2SO_4

In Fig. 4 are shown the linear sweep and cyclic voltammograms obtained for Al-100mM Na_2SO_4 system. Table 2 presents the corrosion parameters calculated by means of potentiodynamic polarization curves recorded at aluminum dissolution in diluted aqueous solutions of 0.1 M Na_2SO_4.

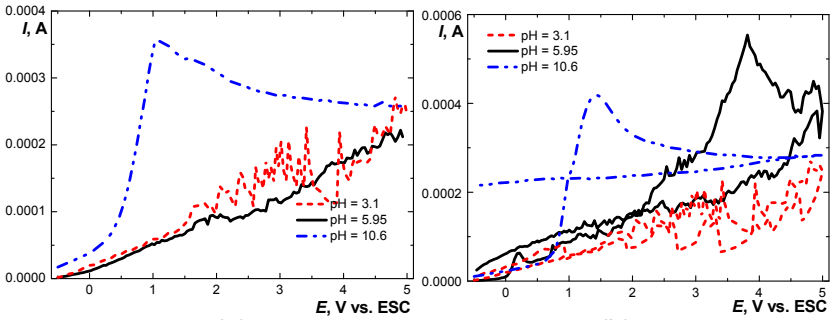

Figure 4. Linear sweep (a) and cyclic (b) voltammograms obtained at different values of pH. Potential ranges: -0.5 – 5 V/ESC and -0.5 – 5.5 -0.5 V/ESC; sweep rate 50 $mV \cdot s^{-1}$; Resolution time 0.8 s, T = 298 K, anode diameter 2.07 mm

Table 2. Corrosion parameters of Al÷100 mM Na_2SO_4 system at different values of pH

Run No.	pH	Potential range	Sweep rate	E_{cor}	$I_{O,\ init}$	R_p	$I_{O,\ Tafel}$	$i_{O,\ Tafel}$
		V vs. ESC	$mV \cdot s^{-1}$	V	A	$\Omega \cdot m^2$	A	$A \cdot m^{-2}$
1	3.10	–0.5 ÷ 5	50	-0.591	$3.418 \cdot 10^{-08}$	0.833	$4.831 \cdot 10^{-08}$	0.014
2	5.95	–0.5 ÷ 5	50	-0.588	$6.541 \cdot 10^{-08}$	0.435	$1.490 \cdot 10^{-07}$	0.044
3	10.60	–0.5 ÷ 5	50	-0.113	$5.837 \cdot 10^{-07}$	0.049	$1.012 \cdot 10^{-06}$	0.301

According to the results presented in Table 2, the most corrosive medium for *Al÷100 mM Na_2SO_4* system is the alkaline one, while in the acid medium, the corrosion current achieves the lowest value. The behavior of aluminum dissolution in aqueous solutions of sodium sulfate is opposed to that of *Al÷3.42 mM NaCl* system, thus emphasizing the influence of the chloride ion onto the dissolution process of aluminum.

Linear sweep and cyclic voltrammograms shown in Fig. 4 support this conclusion. Moreover, the passivation phenomenon at the alkaline pH has been pinpointed. Throughout the potential range where the anode becomes passivated, the mass transfer is the limiting dissolution rate. In acid range and near neutral value of pH, *Al÷100 mM Na_2SO_4* system becomes unstable at potential values higher than 1.5 V when current oscillates strongly.

Iron dissolution in diluted aqueous solution containing NaCl

In Fig. 5a are shown the linear sweep voltammograms obtained at iron dissolution in diluted aqueous solutions of NaCl at various pH values.

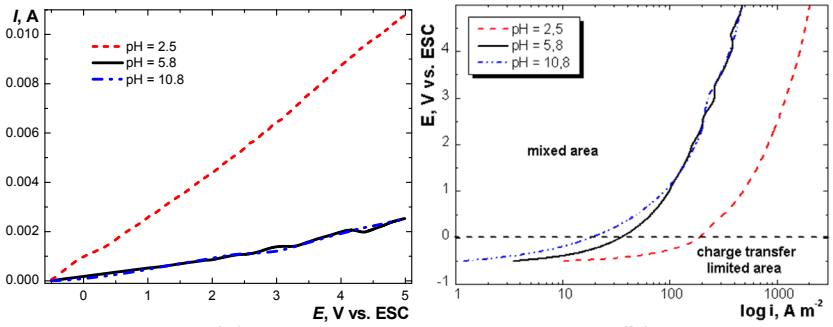

(a) (b)

Figure 5. Linear sweep voltammograms (a) and their semilogarithmic plots (b) at iron dissolution in aqueous solution of NaCl at different pH values. Potential ranges: -0.5 – 5 V/ESC and -0.5 – 5 -0.5 V/ESC; sweep rate 50 mV·s^{-1}; Resolution time 0.8 s, T = 298 K, anode diameter 2.6 mm

Fig. 5b points out two distinct areas on the investigated potential range. Thus, the first part is characteristic to the exchange transfer limiting rate, while the second part corresponds to a mixed area where current density increase accelerates with the increase of the potential values due to a more pronounced influence of mass transport over the dissolution rate.

Fig. 6 presents linear sweep voltammograms and Evans plots obtained at iron dissolution in diluted aqueous solutions of NaCl at different values of scan rate.

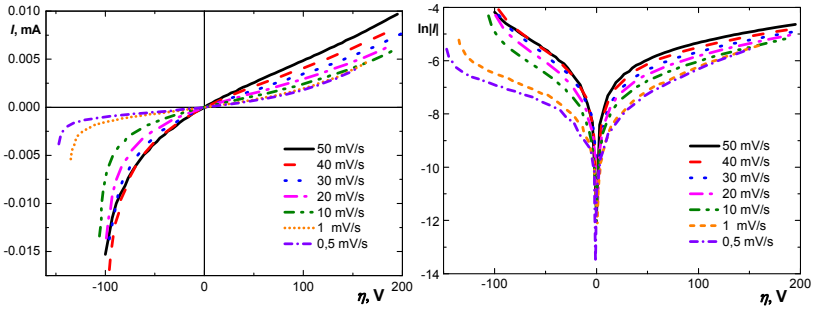

(a) (b)

Figure 6. Current-overpotential (a) and Evans (b) plots corresponding to iron dissolution in aqueous solutions of NaCl at different values of potential sweep rate, pH = 5.8. Potential range: -0.15 – 0.15 V/ESC, T = 298 K, anode diameter 2.6 mm

As in the case of aluminum dissolution, in the presence of chloride ions, iron dissolution takes also place with a positive influence of potential sweep rate over the corrosion current.

The values of corrosion parameters calculated for this system are presented in Table 3.

Table 3. Corrosion parameters of Fe÷3.42 mM NaCl system at different values of pH and sweep rates

Run No.	pH	Potential range	Sweep rate	E_{cor}	$I_{O,\,init}$	R_p	$I_{O,\,Tafel}$	$i_{O,\,Tafel}$
		V vs. ESC	$mV \cdot s^{-1}$	V	A	$\Omega \cdot m^2$	A	$A \cdot m^{-2}$
1	2.54	–0.5 ÷ 5	50	-0.555	$3.09 \cdot 10^{-06}$	0.022	$3.381 \cdot 10^{-06}$	0.637
2	5.80	–0.5 ÷ 5	50	-0.572	$7.35 \cdot 10^{-07}$	0.092	$5.129 \cdot 10^{-07}$	0.097
3	10.8	–0.5 ÷ 5	50	-0.542	$6.90 \cdot 10^{-07}$	0.097	$4.794 \cdot 10^{-07}$	0.090
4	5.8	–0.15 ÷ 0.15	50	-0.572	$7.347 \cdot 10^{-07}$	0.092	$5.129 \cdot 10^{-07}$	0.097
5	5.8	–0.15 ÷ 0.15	40	-0.589	$6.611 \cdot 10^{-07}$	0.102	$4.694 \cdot 10^{-07}$	0.088
6	5.8	–0.15 ÷ 0.15	30	-0.593	$5.720 \cdot 10^{-07}$	0.118	$3.958 \cdot 10^{-07}$	0.075
7	5.8	–0.15 ÷ 0.15	20	-0.593	$4.300 \cdot 10^{-07}$	0.156	$2.827 \cdot 10^{-07}$	0.053
8	5.8	–0.15 ÷ 0.15	10	-0.589	$3.083 \cdot 10^{-07}$	0.218	$2.225 \cdot 10^{-07}$	0.042
9	5.8	–0.15 ÷ 0.15	1	-0.560	$1.804 \cdot 10^{-07}$	0.373	$1.690 \cdot 10^{-07}$	0.032
10	5.8	–0.15 ÷ 0.15	0.5	-0.552	$1.509 \cdot 10^{-07}$	0.446	$1.587 \cdot 10^{-07}$	0.030

It can be noticed that the acid medium is the most corrosive one in case of steel. Also, it is emphasized a similar behavior of iron dissolution at pH = 5.8 and 10.8 respectively, which is supported by the values of corrosion current and polarization resistances as listed in Table 3.

In Fig. 7 is shown the variation of iron dissolution rate in the presence of chloride ions at different values of pH and current potential. Iron dissolution rate is proportional with the potential, the highest values corresponding to the acid values of pH.

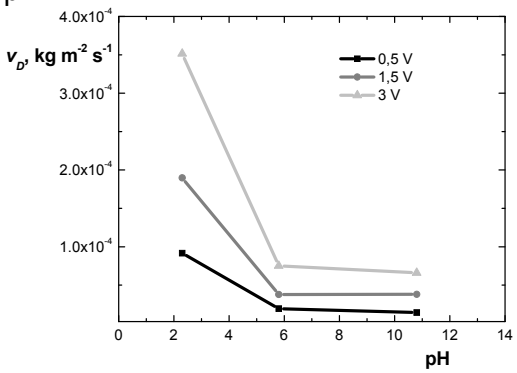

Figure 7. Dependence of iron dissolution rate on solution pH

Iron dissolution in diluted aqueous solution containing Na_2SO_4

Fig. 8 shows linear sweep and cyclic voltammograms measured at iron dissolution in aqueous solution of *100 mM* Na_2SO_4 at various values of pH and potential respectively.

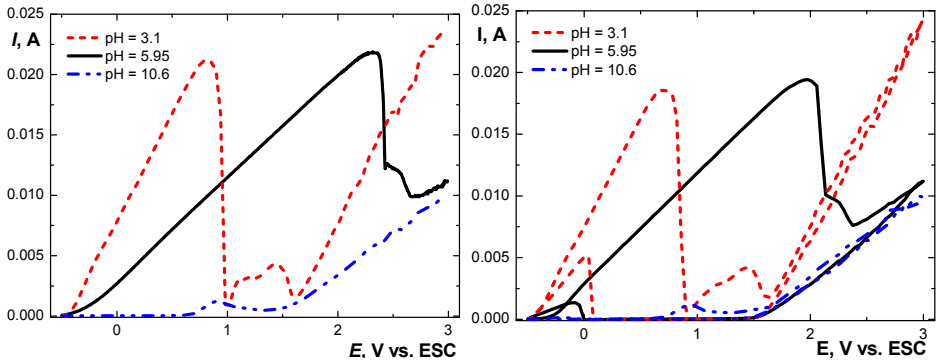

Figure 8. Linear sweep (a) and cyclic (b) voltrammograms obtained at iron dissolution in aqueous solutions of Na_2SO_4 at different values of pH. Potential ranges: -0.5 – 3 V/ESC and -0.5 – 3 -0.5 V/ESC; sweep rate 50 $mV \cdot s^{-1}$; Resolution time 0.8 s, T = 298 K, anode diameter 2.6 mm

It can be noticed the passivation of iron surface at the alkaline pH. Also, the mixed regime step is extended at higher values of the potential.

In Table 4 are presented the corrosion parameters corresponding to iron dissolution in aqueous solutions of *100 mM* Na_2SO_4 at different values of pH. These parameters were determined on the basis of linear sweep voltammograms and Evans plots shown in Fig. 9.

Table 4. Corrosion parameters of Fe÷100 mM Na_2SO_4 system at different values of pH

Run No.	pH	Potential range	Sweep rate	E_{cor}	$I_{O,\ init}$	R_p	$I_{O,\ Tafel}$	$i_{O,\ Tafel}$
		V vs. ESC	$mV \cdot s^{-1}$	V	A	$\Omega \cdot m^2$	A	$A \cdot m^{-2}$
1	3.10	–0.5 ÷ 5	50	-0.616	$3.72 \cdot 10^{-06}$	0.018	$2.677 \cdot 10^{-06}$	0.504
2	5.95	–0.5 ÷ 5	50	-0.522	$8.11 \cdot 10^{-07}$	0.083	$5.026 \cdot 10^{-07}$	0.095
3	10.60	–0.5 ÷ 5	50	-0.569	$9.62 \cdot 10^{-07}$	0.071	$5.943 \cdot 10^{-07}$	0.112

Acid medium favors the corrosion of iron in aqueous solutions of Na_2SO_4. However, compared to the system containing chloride ions, the passivation phenomenon occurs. In case of alkaline pH, the passivation is very strong, being recorded a peak of $1.22 \cdot 10^{-3}$ *A* at *0.9 V*, while in acid medium, the peak reaches the value of $2.1 \cdot 10^{-2}$ *A* at 0.8 V.

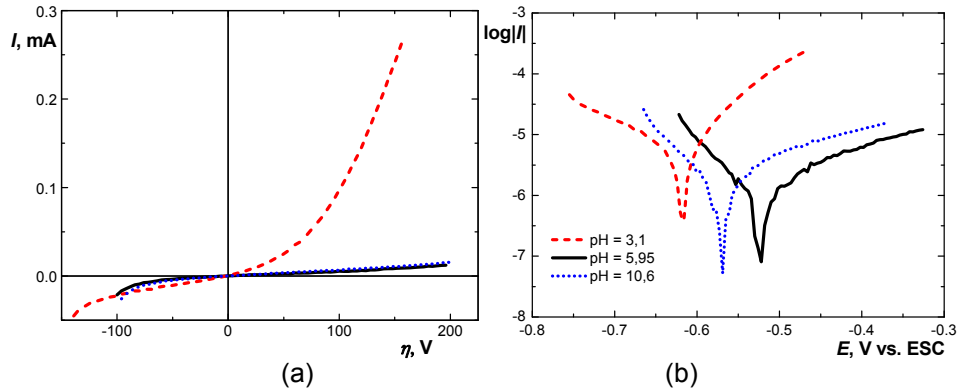

(a) (b)

Figure 9. Current-overpotential (a) and Evans (b) plots corresponding to iron dissolution in aqueous solutions of Na_2SO_4 at different sweep rates. Potential ranges: -0.15 – 0.15 V/ESC, T = 298 K, anode diameter 2.6 mm

CONCLUSIONS

Four different electrochemical systems were voltammetrically characterized. Several studies specific to processes taking place under kinetic and mixed regimes were performed. Thus, parameters such as current density at null potential, heterogeneous constant rate in mixed regime and dissolution rate were determined.

In order to describe the process of anodic dissolution of aluminum and iron respectively in diluted aqueous solutions, potentiodynamic polarization curves were measured on different potential ranges.

Based on linear sweep voltammograms measured on relatively small ranges of potential values, current density at null potential was determined by two different methods. These have allowed comparing the investigated systems in relation to anodic dissolution rate of aluminum and iron respectively at different values of pH, for two different support electrolytes. By widening the investigated potential range from -0.15-0.15 V to -0.5-5V, it was emphasized the influence of mass transport over the global rate of the dissolution rate of both aluminum and iron.

Considering the current values at different potentials, the dissolution rate of the four investigated systems were determined.

It was found that in case of aluminum dissolution in the presence of chloride ion, no passivation phenomenon occurs. At null potential, the alkaline pH favors most the corrosion process, while applying a potential difference, the dissolution process of aluminum in the presence of sulfate ion is influenced by the occurrence of the passivation phenomenon.

In case of iron dissolution into aqueous solutions of NaCl or Na_2SO_4 relatively close values were obtained at certain values of pH. However, in the presence of sulfate ion, the anode becomes passivated.

The obtained results emphasize the positive role played by the chloride ion in both aluminum and iron anodic dissolution processes.

EXPERIMENTAL SECTION

Materials and reagents

Electrode materials used in investigations were made of aluminum (*EN AW-1080A*, composition: *Al* min. *99.5%*, *Si 0.2%*, *Fe 0.2%*, *Zn 0.03*, *Mn 0.03)*, steel (*OL 32*, composition: *Fe* min. *99,14%*, *C* max *0.15*, *Mn* max. *0.6%*, *P* max *0.055%*, *S* max. *0.055%*), stainless steel (*X5CrNi18-10*, composition, *C 0.05%*, *Cr 18%*, *Ni 10 wt%*).

Aqueous solutions of 3.42 mM sodium chloride and 0.1 M sodium sulfate were prepared by dissolving *NaCl* A.R. and $Na_2SO_4 \cdot 10H_2O$ A.R. (Lachner, Czech Republik) into distilled water.

Adjustment of pH of aqueous solution was achieved by using 0.1 N and 1 N solutions of H_2SO_4 and NaOH respectively. These solutions were prepared by dissolving anhydrous NaOH A.R. (Fluka, Germany) and diluting H_2SO_4 98% solution (Merck, Germany) into distilled water.

Experimental Procedures

In order to measure the potentiodynamic polarization curves, the VoltaLab 32 (Radiometer Copenhagen) electrochemical installation, presented in Fig. 10, was employed.

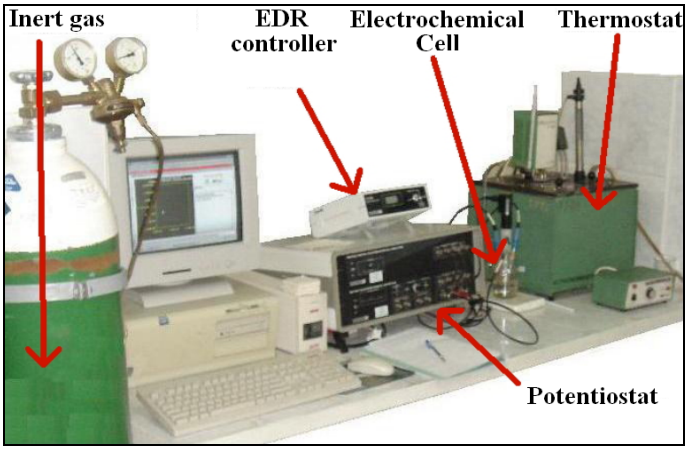

Figure 10. VoltaLab 32 electrochemical system

This electrochemical system is composed of a DEA-322 digital electrochemical analyzer potentiostat, an electrolytic cell with three electrodes provided with thermal coating and gas-sparging system, an IMT 102 data interface connected to a computer operated with Volta Master software.

CTV 101 (Radiometer Copenhagen) was employed for operating the rotating electrode in the range of 0-5000 RPM. The thermostating system consisted of a 657 MTA Kutesz controlled by 1031 MTA Kutesz regulator. For removing air from the electrolyte solution, a nitrogen gas bottle was used.

Cylindrical electrodes were fixed into Teflon (PTFE) supports for mechanical and electrical connection to the rotating device.

The electrolytic cell is composed of three electrodes according to a standard geometry and is provided with thermal coating. The three-electrode geometry varied as a function of the studied systems. Thus, there were employed discs of aluminum (disc of *2.07 mm*) or steel (disc of *2.6 mm*) as working electrode, a saturated calomel electrode as reference electrode, and a platinum electrode as counter-electrode. A volume of *30 mL* of electrolyte solution was used in the experimental investigations [21-23].

During the preliminary experiments it was found that the voltammograms of the investigated systems are highly reproducible.

ACKNOWLEDGMENTS

This work was supported by CNCSIS-UEFISCSU, PN II-RU No. 52/2010, COD 44.

REFERENCES

1. X.M. Chen, G.H. Chen, P.L. Yue, *Chemical Engineering Science*, **2002**, *57*, 2449.
2. P.K. Holt, G.W. Barton, M. Wark, C.A. Mitchell, *Colloids and Surfaces A: Physicochemical and Engineering Aspects*, **2002**, *211*, 233.
3. P.K. Holt, G.W. Barton, C.A. Mitchell, “6th World Congress of Chemical Engineering”, Conference Media CD (paper 518), Melbourne, Australia, **2001**, p. 518.
4. P. Canizares, M. Carmona, J. Lobato, F. Martinez, M.A. Rodrigo, *Industrial & Engineering Chemistry Research*, **2005**, *44*, 4178.
5. P. Canizares, F. Martınez, C. Jimenez, J. Lobato, M.A. Rodrigo, *Industrial & Engineering Chemistry Research*, **2006**, *45*, 8749.
6. P. Canizares, C. Jimenez, F. Martınez, C. Saez, M.A. Rodrigo, *Industrial & Engineering Chemistry Research*, **2007**, *46*, 6189.
7. M.Y.A. Mollah, P. Morkovsky, J.A.G. Gomes, M. Kesmez, J. Parga, D.L. Cocke, *Journal of Hazardous Materials*, **2004**, *114*, 199.
8. C. Noubactep, A. Schoner, *Journal of Hazardous Materials*, **2010**, *175*, 1075.
9. G. Mouedhen, M. Feki, M. de Petris Wery, H.F. Ayedi, *Journal of Hazardous Materials*, **2008**, *150*, 124.

10. M.S. Secula, I. Cretescu, S. Petrescu, *Desalination*, **2011**, *277*, 227.
11. R. Stefec, “Corrosion data from polarization measurements”, Ellis Horwood, New York, **1990**.
12. T. Visan, “Electrochimie şi coroziune pentru doctoranzii” ELCOR, vol. 1, Printech, Bucureşti, **2002**.
13. M. Stern, A.L. Geary, *Journal of the Electrochemical Society*, **1957**, *104*, 559.
14. H. Uhlig, “Corrosion and Corrosion Control”, John Wiley&Sons Inc., New York, **1971**.
15. F. Mansfeld, “The polarization resistance technique for measuring corrosion currents, Advances in Corrosion Science and Technology”, vol. VI, Plenum Press, New York, **1976**.
16. M. Stern, *Corrosion*, **1958**, *14*, 440.
17. J.M. West, “Basic corrosion and oxidation”, Ellis Horwood, New York, **1990**.
18. S. Petrescu, M.S. Secula, *Revista de Chimie*, **2005**, *56*, 977.
19. D.D. Macdonald, *Journal of the Electrochemical Society*, **1978**, *125*, 1443.
20. J.C. Donini, J. Kan, J. Szynkarczuk, T.A. Hassan, K.L. Kar, *Canadian Journal of Chemical Engineering*, **1994**, *72*, 1007.
21. S. Petrescu, M.S. Secula, I. Cretescu, Gh. Nemtoi, *Revista de Chimie*, **2009**, *60*, 462.
22. Gh. Nemtoi, M.S. Secula, I. Cretescu, S. Petrescu, *Revue Roumaine de Chimie*, **2007**, *52*, 655.
23. Gh. Nemtoi, M.S. Secula, I. Cretescu, S. Petrescu, *Revista de Chimie*, **2007**, *55*, 1216.